



Science Arts & Métiers (SAM)

is an open access repository that collects the work of Arts et Métiers Institute of Technology researchers and makes it freely available over the web where possible.

This is an author-deposited version published in: <https://sam.ensam.eu>
Handle ID: <http://hdl.handle.net/10985/18619>

To cite this version :

Xavier COLIN - Nonempirical Kinetic Modeling of Non-fickian Water Absorption Induced by a Chemical Reaction in Epoxy-Amine Networks - 2018

Any correspondence concerning this service should be sent to the repository

Administrator : scienceouverte@ensam.eu



Nonempirical Kinetic Modeling of Non-fickian Water Absorption Induced by a Chemical Reaction in Epoxy-Amine Networks

Xavier Colin

Abstract In the last two decades, several studies made in our laboratory have shown that hydrolytic reactions may occur during water absorption and may be responsible for behavioral deviations from the classical Fick's law in epoxy-amine networks. On one hand, water is chemically consumed by specific groups initially present in the repetitive structural unit (e.g., unreacted epoxies and amides) or formed by oxidation under operating conditions. On the other hand, water establishes strong molecular interactions (hydrogen bonds) with new highly polar groups resulting from hydrolysis (alcohols and acids). Due to both contributions, the kinetic curves of water absorption no longer tend towards an equilibrium value, i.e., a final saturation plateau, but display a slow and continuous increase over time in the water mass uptake. On this basis, a diffusion/reaction model has been developed for predicting such a peculiar water sorption behavior. In addition, the classical Henry's law has been modified for describing the changes in boundary conditions during the course of the hydrolytic reaction. This chapter provides an overview of the recent theoretical advances made in this field and demonstrates, through two case studies, the good predictive value of the kinetic modeling approach set up in our laboratory.

Keywords Epoxy-amine networks • Water absorption • Hydrolysis • Fick's law deviation • Kinetic modeling

1 Introduction

Epoxy-amine networks are widely used in many industrial fields, such as aeronautics and space, automotive industry, nuclear energy, building and civil engineering, as matrices of fiber reinforced composite materials, structural adhesives of

X. Colin (✉)

Laboratoire PIMM, Arts et Métiers ParisTech, 151 Boulevard de L'Hôpital,
75013 Paris, France

e-mail: xavier.colin@ensam.eu

bonded assemblies, but also protective coatings, in particular paintings, varnishes and lacquers. Many studies have been conducted for tentatively elucidating their physical and chemical aging mechanisms and for evaluating their long-term durability under the combined effects of various environmental stresses such as temperature, UV and ionizing radiations, oxygen, water, etc. [1–3].

These polymers are known to be very sensitive to moisture. First of all, they can absorb large amounts of water due to the presence of highly polar groups (hydroxyls for example) in their repetitive structural unit, which establish strong molecular interactions (hydrogen bonds) with water molecules. That is the reason why they undergo an important external plasticization when they are initially in the glassy state. As an example, an ideal DGEBA-DDM network absorbs more than 2 wt% of water in 100% RH at 25 °C, which reduces its glass transition temperature T_g by about 36 °C [4].

In addition, epoxy-amine networks can undergo a hydrolysis reaction when they contain specific chemical groups known to be reactive with water. These latter can be initially present in the repetitive structural unit as, for instance, amides in networks based on amidoamine hardeners [5] or unreacted epoxies in non-ideal networks [6]. But, they may also be formed by a radical chain oxidation reaction activated by external factors (e.g., increase in temperature, UV or ionizing radiation, or chemical reagent acting as a radical initiator) under operating conditions. These chemical groups are then amides and esters resulting from the oxidation of amino- and oxy-methylenes respectively [7]. In both cases, hydrolysis will lead to the formation and accumulation of new hydroxyl groups (alcohols and acids) and consequently, to significant changes in water transport properties in epoxy-amine networks.

This chapter proposes to review all these physico-chemical mechanisms and to derive, from these latter, a general kinetic model capable of predicting two examples of behavioral deviations from the classical Fick's law reported in the literature for epoxy-amine networks.

2 Water Absorption in the Absence of Hydrolysable Groups

In the absence of hydrolysable groups in epoxy-amine networks, water absorption obeys the classical Fick's second law [6, 8, 9]. A typical kinetic curve of water absorption is plotted versus the square root of time in Fig. 1a. Two time domains can be clearly distinguished:

- I. The transient regime during which the water mass uptake m (expressed in wt %) increases linearly with the square root of time. The slope of this straight line allows the coefficient D of water diffusion to be determined. During this period, water is heterogeneously distributed in the sample thickness as schematized in Fig. 1b.

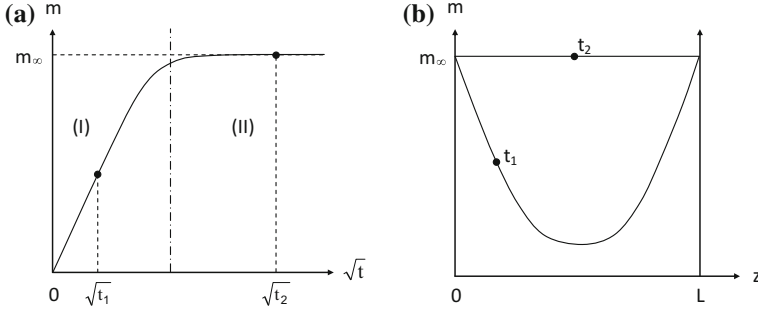


Fig. 1 **a** Typical kinetic curve of water absorption for a Fick's diffusion process. **b** Water gradient in the sample thickness at two different times of exposure

- II. The final saturation plateau for which m has reached its maximum value m_∞ throughout the sample thickness (for the exposure conditions under study). Thenceforth, water is homogeneously distributed throughout the sample thickness.

The equilibrium mass uptake m_∞ , mass fraction μ_∞ and concentration C_∞ of absorbed water in the polymer sample are linked by the following relationships:

$$\mu_\infty = \frac{m_\infty}{1 + m_\infty} \quad \text{and} \quad C_\infty = \frac{m_\infty}{18} \quad (\text{expressed in mol g}^{-1}) \quad (2.1)$$

2.1 Equilibrium Properties

Since water is far below its critical point ($T_C = 647$ K), the pertinent environmental parameter is the water activity a . Let us remember that for humid atmospheres:

$$a = \frac{p_V}{p_{VS}} = \frac{RH}{100}, \quad (2.2)$$

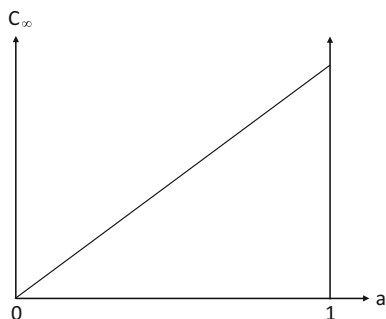
where p_V and p_{VS} are respectively the water partial pressure in the atmosphere and the saturated vapor pressure of water.

In the absence of hydrolysable groups in epoxy-amine networks, C_∞ varies linearly with a over the whole activity range (Fig. 2). In other words, C_∞ obeys the classical Henry's law [10]:

$$C_\infty = H a, \quad (2.3)$$

where H is almost independent of temperature.

Fig. 2 Typical sorption isotherm of Henry's type



2.2 Origin of Hydrophilicity

In the 1980s, many authors have tried to relate the polymer hydrophilicity to the available free volume [11–14], but such theory fails in explaining why free-volume-rich organic substances, such as liquid hydrocarbons and silicone rubbers, are hydrophobic. Today, it seems clear that hydrophilicity is essentially linked to the molecular interactions between water molecules and polar groups in the polymer matrix. In a first approach, m_{∞} can be roughly estimated from Hildebrandt's solubility parameter δ . Indeed this latter, which is directly related to the chemical structure of the polymer, gives access to polymer-solvent interactions. It can be written:

$$\delta = \frac{F}{V} \quad (2.4)$$

with F the molar attraction constant and V the molar volume of the polymer.

According to Van Krevelen's theory [15], both quantities are molar additive functions, i.e., they can be calculated by summing the molar contributions of the different chemical groups composing the repetitive structural unit:

$$F = \sum F_i \quad \text{and} \quad V = \sum V_i \quad (2.5)$$

Table 1 summarizes the values of F_i and V_i proposed by Small [16], Van Krevelen [17], Hoy [18] and Fedors [19] for usual chemical groups.

The literature values of m_{∞} in 100% RH at 25 °C of different polymers have been compiled and plotted versus δ (calculated from Eqs. 2.4 and 2.5) in the log-log diagram of Fig. 3.

A correlation is clearly observed between both quantities. It can be written:

$$m_{\infty} = 7.1 \times 10^{-10} \delta^{6.86} \quad (2.6)$$

Table 1 Molar contributions to F [16–18] and V [19] of usual chemical groups. Ph designates an aromatic ring

Group	F_i ($\text{J}^{1/2} \text{cm}^{3/2} \text{mol}^{-1}$)	V_i ($\text{cm}^3 \text{mol}^{-1}$)
–CH ₃	370	33.5
–CH ₂ –	275	16.1
>CH–	115	–1
>C<	15	–19.5
–Ph–	1680	89.4
–O–	200	3.8
>N–	125	–9
–NH ₂	490	19.2
–CO–	560	10.8
–O–CO–	590	18
–O–CO–O–	760	22
–CO–O–CO–	960	30
–NH–CO–	1110	9.5
–CO–OH	825	28.5
–OH	610	10
–SO ₂ –	845	19.6

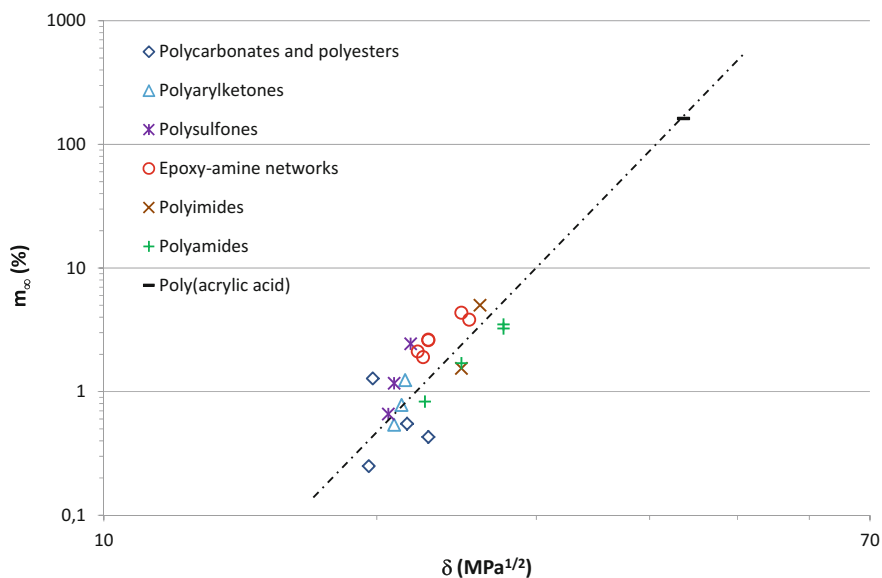


Fig. 3 Equilibrium water mass uptake (in 100% RH at 25 °C) versus solubility parameter for 24 polymers

Epoxy-amine networks are moderately polar polymers ($22 < \delta < 25 \text{ MPa}^{1/2}$). They absorb typically between 1 and 4 wt% of water in 100% RH at 25 °C.

2.3 Effect of Structure on Hydrophilicity

According to Van Krevelen [15], C_∞ would be a molar additive function, i.e., each chemical group of the repetitive structural unit would be characterized by a molar contribution to hydrophilicity H_i (in mole of water per mole of group) independent of its chemical neighbors:

$$C_\infty = \left(\frac{18}{M_{\text{RSU}}} \sum H_i \right) \times \frac{\text{HR}}{100}, \quad (2.7)$$

where M_{RSU} is the molar mass of the repetitive structural unit. Table 2 summarizes the values of H_i determined by Barrie [20] for usual chemical groups in 100% RH at 25 °C. On this basis, three main categories of chemical groups can be defined:

- Apolar groups, such as aromatic and aliphatic hydrocarbon structures, which have a negligible contribution to hydrophilicity: $H_i \approx 0 \text{ mol/mol}$;
- Moderately polar groups, for instance ethers, ketones and esters, which have a relatively low contribution to hydrophilicity: $H_i = 0.1\text{--}0.3 \text{ mol/mol}$;
- And highly polar groups, for instance acids, amides, and alcohols, which establish intense molecular interactions with water molecules (hydrogen bonds) and absorb typically $H_i = 1\text{--}2 \text{ mol/mol}$.

Equation 2.7 can be used for estimating the orders of magnitude of C_∞ for the main polymer families. In contrast, this approach fails in predicting the hydrophilicity variations within a same polymer family which displays large concentration differences in polar groups, such as epoxy-amine networks [6] and polysulfones [21]. Indeed in these two latter, it has been found that C_∞ does not

Table 2 Molar contributions to hydrophilicity (in moles of water per mole of group) of usual chemical groups in 100% RH at 25 °C [20]. Ph designates an aromatic ring

Polarity	Group	H_i (mol/mol)
--	-CH ₃	0.00005
	-CH ₂ -	
	>CH-	
	-Ph-	
+	-O-	0.1
	-CO-	0.2
	-O-CO-	0.3
+++	-CO-OH	1.3
	-CO-NH-	2
	-OH	2

increase linearly but exponentially with the concentration of polar groups (i.e., hydroxyls and sulfones, respectively).

Gaudichet-Maurin et al. [21] have proposed a theory for tentatively explaining such a behavior. According to these authors, an hydrophilic site would not be a single but a pair of polar groups having to satisfy some geometric requirements (in particular an optimal distance between them) in order to establish a double hydrogen bond with a water molecule. As schematized in Fig. 4, the probability of finding two polar groups at this optimal distance would increase exponentially with their concentration, which could effectively explain the mathematical shape observed experimentally for the curve: $C_{\infty} = f([\text{Polar group}])$.

More recently, Courvoisier [22] has compiled the literature values of C_{∞} in 100% RH at 25 °C of different polymers and plotted them versus the concentration of the most polar group in the repetitive structural unit (Fig. 5). It can be seen that all the points are placed around only three master curves, which allows to distinguish three main categories of polar groups: slightly (esters and carbonates), moderately (aryl ketones, amides and imides), and highly polar groups (hydroxyls and sulfones). Thus, it appears clearly that all carbonyl groups do not display the same behavior. The lower contribution to hydrophilicity of esters and carbonates had been already reported in the literature by several other authors, for instance in reference [23].

Since these three curves display an exponential shape, it can be assumed that the previous theory can be generalized to all polymers. A general semi-empirical structure/ C_{∞} relationship can be proposed:

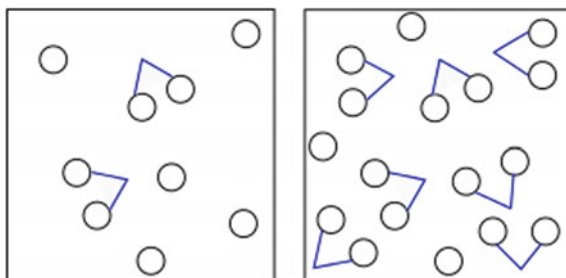
$$C_{\infty} = A \text{Exp}\{B[\text{Polar group}]\} \times \frac{\text{HR}}{100}, \quad (2.8)$$

where A is almost independent of the chemical structure: $A = (1.23 \pm 0.41) 10^{-1} \text{ mol.L}^{-1}$ for all polymers. In contrast, B is an increasing function of the group polarity.

In fact, B is found to be proportional to the “elemental” solubility parameter of the polar group under consideration:

$$B = (6.7 \pm 1.0) 10^{-3} \times \delta \quad (2.9)$$

Fig. 4 Schematization of the probability increase of finding two polar groups at an optimal distance for establishing a double hydrogen bond with a water molecule o: polar group. \wedge : water molecule



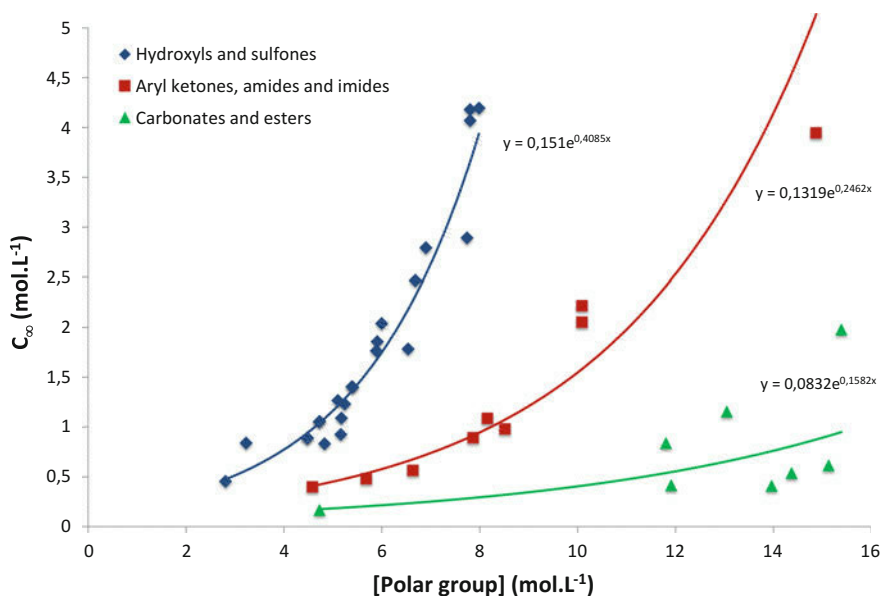


Fig. 5 Equilibrium water concentration (in 100% RH at 25 °C) versus polar group concentration for 40 polymers

Table 3 Solubility parameters of common chemical groups. Ph designates an aromatic ring

Polarity	Group	δ (MPa ^{1/2})
--	-CH ₃	16.8 ± 2.1
	-CH ₂ -	
	>CH-	
	-Ph-	
+	-O-	22.8
	-O-CO-	27.4 ± 0.1
	-CO-O-CO-	
++	-CO-	32.6 ± 2.3
	-CO-H	
	-CO-NH ₂	
	-CO-NH-	
+++	-SO ₂	50.4 ± 2.5
	-OH	

Table 3 summarizes the values of δ calculated for usual chemical groups from the values of cohesive energy E_{coh} and molar volume V , reported respectively by Fedors [19] and Hoy [18], and applying the well-known relationship:

$$\delta = \left(\frac{E_{\text{coh}}}{V} \right)^{1/2} \quad (2.10)$$

2.4 Effect of Structure on Diffusivity

In contrast, the relationships between polymer structure and water diffusivity are far from being totally elucidated. Thominet et al. [24] have observed that D is a decreasing function of hydrophilicity in different polymer families, for instance in epoxy-amine networks, aromatic polysulfones, and polyester-styrene networks, but also in a series of polyethylenes differing by their initial concentration of oxygenated groups (pre-oxidation). This dependence shows that the diffusion rate is slowed down by the molecular interactions between water molecules and polar groups in the polymer matrix. A three-step scheme has been proposed [6] to describe such a diffusion mechanism (Fig. 6). According to this scheme, water diffusion is not highly influenced by the macromolecular mobility if the dissociation of the water-polymer complex (I) is slower than the water migration between neighboring hydrophilic sites (II).

Courvoisier [22] has compiled the literature values of water permeability P in 100% RH at 25 °C of different polymers and plotted them versus the concentration of the most polar group in the repetitive structural unit (Fig. 7). It can be seen that P is of the same order of magnitude for all polymers. The data scattering within a same polymer family can be explained by the small effect on P of secondary structural factors at higher scales, e.g., differences in crosslinking density in networks, differences in crystallinity ratio and crystalline lamellae thickness in semi-crystalline polymers, etc., which modify the tortuosity of the water diffusion path. In a first approximation, it can be written:

$$P = C_{\infty} \times D = 10^{-9.7 \pm 0.7} \quad (\text{expressed in mol m}^{-1} \text{ s}^{-1}) \quad (2.11)$$

In other words, D is inversely proportional to C_{∞} .

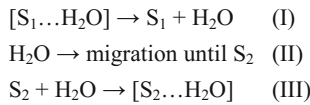


Fig. 6 Three-step mechanism for water diffusion into polymer matrices [6]. S_1 and S_2 designate two neighboring hydrophilic sites and $[S_1 \dots H_2O]$ a hydrogen bonded water-polymer complex

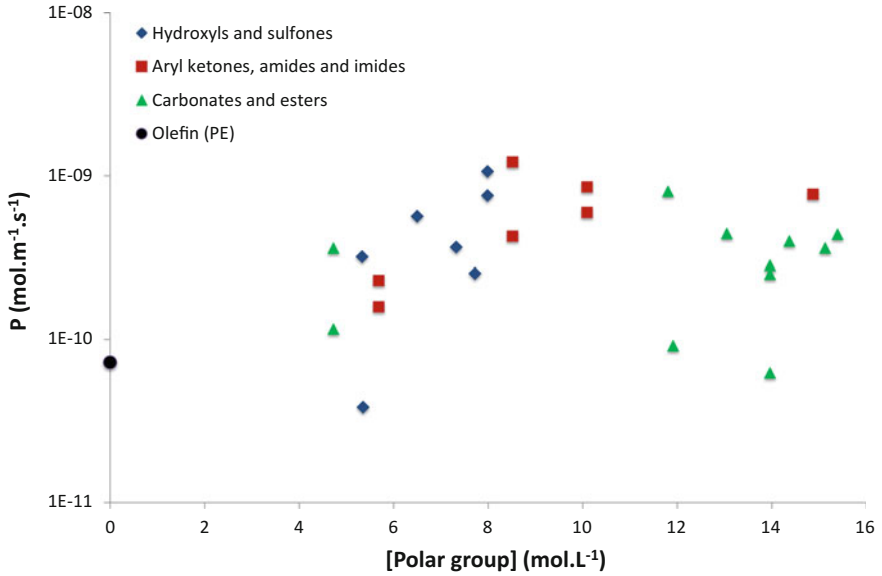
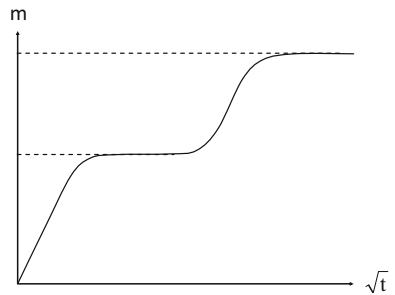


Fig. 7 Water permeability (in 100% RH at 25 °C) versus polar group concentration for 27 polymers

Fig. 8 Typical kinetic curves of water absorption for a Langmuir's diffusion process



3 Water Absorption in the Presence of Hydrolysable Groups

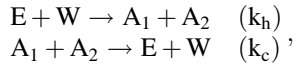
In the presence of hydrolysable groups in epoxy-amine networks, different behavioral deviations from the classical Fick's law have been reported in the literature. Some of them are clearly related to chemical modifications.

In the case of non-ideal networks containing unreacted epoxy groups, water absorption displays a two-step behavior (Fig. 8) often classified in the categories of

calculated from a balanced equation, expressing that the change over time t in water concentration C in an elementary sublayer located at the depth z beneath the sample surface is the difference between the water supply by diffusion (according to the Fick's second law) and the water consumption by the chemical reaction:

$$\frac{\partial C}{\partial t} = D \frac{\partial^2 C}{\partial z^2} - r(C) \quad (4.1)$$

The mathematical expression of the water consumption rate is deduced from a kinetic analysis of the reversible hydrolysis scheme:



where E , W , A_1 , and A_2 account respectively for hydrolysable groups, water, and hydrolysis products. k_h and k_c are the respective rate constants of the hydrolysis and condensation reactions. The water consumption rate can be written as:

$$r(C) = -\frac{dC}{dt} = k_h[E] C - k_c[A_1][A_2] \quad (4.2)$$

The corresponding gradients in the sample thickness of hydrolysable groups and hydrolysis products are determined from complementary equations:

$$\frac{d[E]}{dt} = -k_h[E] C + k_c[A_1][A_2] \quad (4.3)$$

$$\frac{d[A_1]}{dt} = \frac{d[A_2]}{dt} = k_h[E] C - k_c[A_1][A_2] \quad (4.4)$$

The system of Eqs. 4.1–4.4 has been solved simultaneously in space (z) and time (t) using the numerical algorithms recommended for problems of chemical kinetics in the literature. Let us note that these algorithms are already implemented in the commercial MATLAB® software under the names of ODE23 s and ODE23 tb. The initial (throughout the sample thickness) and boundary conditions (at the sample surface) used for this resolution are recalled below:

- At $t = 0$ and any z : $C(z, 0) = 0$, $[E](z, 0) = [E]_0$ and $[A_1](z, 0) = [A_2](z, 0) = 0$.
- When $t > 0$, at $z = 0$ and L : $C(0, t) = C(L, t) = C_S(t)$.

Let us remember that, due to the hydrolysis reaction, the water concentration C_S at the sample surface is no longer a constant but it is an increasing function of time. It can be determined from Eq. 2.8 if the total concentration of highly polar groups (i.e., hydroxyls) at any time t is known. The initial value of C_S corresponds to the equilibrium water concentration C_∞ that should be found if the epoxy-amine network under consideration did not contain hydrolysable groups. The increase in C_S against time of exposure can be determined by introducing the solution of Eq. 4.4

into Eq. 2.8. Indeed, for the two hydrolysis examples reported in Fig. 9, this latter writes:

$$C_S = A \text{Exp}\{B [\text{OH}]\} \quad (4.5)$$

with $A = 1.51 \times 10^{-1} \text{ mol L}^{-1}$ and $B = 4.09 \times 10^{-1} \text{ L mol}^{-1}$. If considering the definition of C_∞ , this equation can be rewritten:

$$C_S = C_\infty \text{Exp}\{B([\text{OH}] - [\text{OH}]_0)\} \quad (4.6)$$

Since hydroxyl groups (OH) come from alcohols (Al) and acids (Ac), it comes finally:

$$C_S = C_\infty \text{Exp}\{B([\text{Al}] - [\text{Al}]_0)\} \times \text{Exp}\{B([\text{Ac}] - [\text{Ac}]_0)\} \quad (4.7)$$

In addition, always due to the hydrolysis reaction, the coefficient of water diffusion D through the sample thickness is no longer a constant but a decreasing function of time. It can be determined from Eq. 2.11 through replacing C_∞ by C_S . The initial value of D corresponds to the coefficient of water diffusion D_0 that should be found if the epoxy-amine network under consideration did not contain hydrolysable groups. Since the water permeability is independent of the concentration of polar groups (Eq. 2.11), it can be written:

$$C_\infty \times D_0 = C_S \times D \quad (4.8)$$

If considering Eq. 4.7, it comes finally:

$$D = \frac{D_0}{\text{Exp}\{B([\text{Al}] - [\text{Al}]_0)\} \times \text{Exp}\{B([\text{Ac}] - [\text{Ac}]_0)\}} \quad (4.9)$$

As said before, the local value of the water mass uptake at the depth z beneath the sample surface is the sum of two contributions: water diffusion and water consumption:

$$dm(z,t) = \frac{18}{\rho} \left(C + \int_0^t r(C) dt \right) \quad (\text{expressed in } \%) \quad (4.10)$$

where ρ is the initial polymer density. The global value of the water mass uptake is simply deduced by summing the local values of dm throughout the thickness L of the semi-infinite plate:

$$m(t) = \frac{1}{L} \int_0^L dm(z, t) dz \quad (\text{expressed in } \%) \quad (4.11)$$

5 Application to Two Case Studies

The validity of the kinetic model described in the previous paragraph has been checked for the two hydrolysis examples reported in Fig. 9. Experimental data have been recovered from two distinct research studies [6, 27].

In the case of non-ideal networks containing unreacted epoxy groups, hydrolysis products are diols, therefore $[A_1] = [A_2] = [AI]$ and $[Ac] = [Ac]_0 = 0$. As an example, the simulations of the kinetic curves of water absorption in 100% RH at 50 °C of DGEBD-ETHA networks only differing by their initial concentrations of unreacted epoxy groups are reported in Fig. 10. These networks were synthesized from DGEBD/ETHA mixtures with different $r = \text{amine/epoxy}$ functional ratios [6].

A satisfactory agreement can be observed between theory and experiment. The values of the rate constants k_h and k_c and the coefficient of water diffusion D_0 used for these simulations are specified in Table 4.

On one hand, it is checked that the rate constants take almost the same values in all simulations. At 50 °C, their average values are:

$$k_h = 3.4 \times 10^{-8} \text{ L mol}^{-1} \text{ s}^{-1} \quad \text{and} \quad k_c = 1.5 \times 10^{-8} \text{ L mol}^{-1} \text{ s}^{-1}$$

Thus, it is found that: $k_h \approx 2 \times k_c$. In other words, hydrolysis of epoxy groups is favored over diols condensation for long periods of exposure.

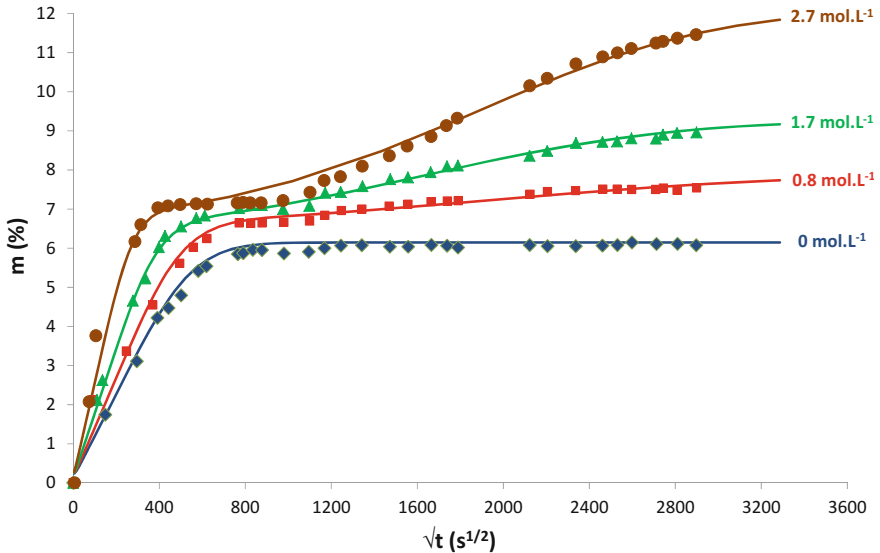


Fig. 10 Kinetic curves of water absorption in 100% RH at 50 °C of non-ideal DGEBD-ETHA networks. Comparison between theory (*solid curves*) and experiments (*symbols*). The concentrations of unreacted epoxies are mentioned next to the curves

Table 4 Rate constants and coefficient of water diffusion used for simulating the kinetic curves of Fig. 10

$[E]_0$ (mol L ⁻¹)	k_h (L.mol ⁻¹ s ⁻¹)	k_c (L mol ⁻¹ s ⁻¹)	D_0 (m ² s ⁻¹)
0.0	–	–	2.5×10^{-12}
0.8	3.0×10^{-8}	1.9×10^{-8}	3.0×10^{-12}
1.7	3.8×10^{-8}	1.1×10^{-8}	5.0×10^{-12}
2.7	3.3×10^{-8}	1.5×10^{-8}	1.0×10^{-11}

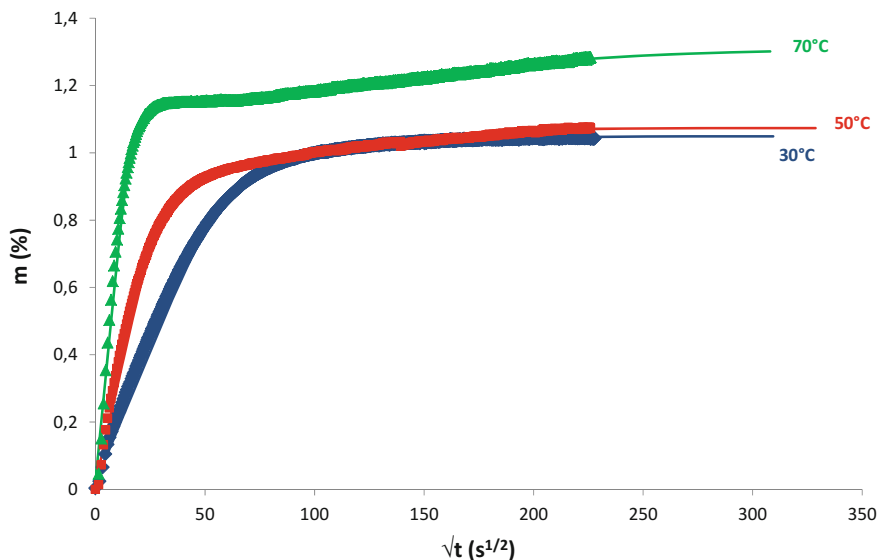


Fig. 11 Kinetic curves of water absorption in 50% RH at 30, 50 and 70 °C of an ideal DGEBA-PAA network. Comparison between theory (*solid curves*) and experiments (*symbols*). The temperatures of exposure are mentioned next to the curves

On the other hand, as expected, the coefficient of water diffusion is a decreasing function of the network polarity. Indeed, D_0 is equal to $2.5 \times 10^{-12} \text{ m}^2 \text{ s}^{-1}$ for the ideal network with an initial concentration of hydroxyl groups of $[\text{OH}]_0 = 8.0 \text{ mol L}^{-1}$, whereas it increases up to $1.0 \times 10^{-11} \text{ m}^2 \text{ s}^{-1}$ for the least ideal network having an initial concentration of hydroxyl groups of $[\text{OH}]_0 = 6.2 \text{ mol L}^{-1}$.

In the case of ideal networks containing amide groups, hydrolysis products are acids and amines, therefore $[A_1] = [\text{Ac}]$, $[A_2] = [\text{Am}]$, and $[\text{Al}] = [\text{Al}]_0$. As an example, the simulations of the kinetic curves of water absorption in 50% RH at 30, 50, and 70 °C of a DGEBA-PAA network are reported in Fig. 11. PAA is a complex amidoamine hardener resulting from the condensation of fatty acids with polyamines (mostly triethylenetetramine) [27].

Table 5 Rate constants and coefficient of water diffusion used for simulating the kinetic curves of Fig. 11

T (°C)	k_h (L mol ⁻¹ s ⁻¹)	k_c (L mol ⁻¹ s ⁻¹)	D_0 (m ² s ⁻¹)
30	6.5×10^{-6}	1.7×10^{-4}	5.0×10^{-13}
50	9.5×10^{-6}	1.5×10^{-4}	2.0×10^{-12}
70	9.5×10^{-6}	1.0×10^{-4}	6.0×10^{-12}

Here also, a satisfactory agreement can be observed between theory and experiment. The values of the rate constants k_h and k_c and the diffusion coefficient D_0 used for these simulations are specified in Table 5.

On one hand, it can be seen that the rate constants are almost independent of temperature. In fact, k_c displays the same order of magnitude as in aliphatic polyamides, e.g., in PA66 [29]. In contrast, k_h is about two decades higher in the epoxy-amidoamine network under consideration than in PA 66. Unfortunately, structure/rate constants relationships are not well known yet in this domain. It is thus too premature to give an explanation.

On the other hand, the values of the coefficient of water diffusion are in very good agreement with those usually reported in the literature for ideal epoxy-amine networks [30]. It is found that D_0 obeys an Arrhenius law with a pre-exponential factor of $1.5 \times 10^{-3} \text{ m}^2 \text{ s}^{-1}$ and an activation energy of 54.9 kJ mol⁻¹.

6 Conclusions

A nonempirical kinetic model has been elaborated for predicting the non-Fickian water absorption induced by a reversible hydrolysis reaction in epoxy-amine networks. This model couples water diffusion and its consumption by the chemical reaction in a system of three differential equations, and takes into account the changes in network hydrophilicity due to the formation of new highly polar groups (alcohols and acids). Its validity has been successfully checked from the experimental results of two case studies conducted in the last two decades in our laboratory.

This model gives access to kinetic parameters (rate constants of hydrolysis and condensation, and coefficient of water diffusion) that are hardly accessible experimentally. The values found for the coefficient of water diffusion are in very good agreement with those already reported in the literature for ideal epoxy-amine networks. In contrast, the values obtained for the rate constants are still questionable. No doubt, these latter have to be the object of a specific study devoted to the humid aging of a large series of epoxy-amine networks containing a well-known concentration of hydrolysable groups after synthesis, but also after storage at room temperature (in particular, in a completely dry atmosphere).

...References

1. Colin X, Verdu J (2011) Thermooxidative and thermohydrolytic aging of organic composite matrices. In: Song DB (ed) Resin composites: properties, production and applications, Chap 7. Nova Science Publishers, New York, pp 255–298
2. Colin X, Verdu J (2012) Aging of organic matrix composite materials. In: Nicolais L, Borzacchiello A, Lee Song SM (eds) Wiley Encyclopedia of composites, 2nd edn, Chap 4. Wiley, New York, pp 35–49
3. Colin X, Verdu J (2014) Humid ageing of organic matrix composites. In: Davies P, Rajapakse YDS (eds) Solid mechanics and its applications 208: durability of composites in a marine environment, Chap 3. Springer, Dordrecht, pp 47–114
4. Bellenger V, Verdu J, Morel E (1989) Structure-properties relationships for densely crosslinked epoxy-amine systems based on epoxide or amine mixtures. Part 2: Water absorption and diffusion. *J Mater Sci* 24:63–68
5. Abdelkader AF, White JR (2005) Water absorption in epoxy resins: The effects of the crosslinking agent and curing temperature. *J Appl Polym Sci* 98(6):2544–2549
6. Tcharkhtchi A, Bronnec Y, Verdu J (2000) Water absorption characteristics of diglycidylether of butane diol-3,5-diethyl-2,4-diaminotoluene networks. *Polymer* 41(15):5777–5785
7. Colin X, Fayolle B, Cinquin J (2016) Further progress in the kinetic modelling of the thermal oxidation of epoxy-diamine matrices. *Mater Tech* 104(2):202
8. Li L, Yu Y, Wu Q, Zhan G, Li S (2009) Effect of chemical structure on water sorption of amine-cured epoxy resins. *Corros Sci* 51:3000–3006
9. Perrin FX, Nguyen MH, Vernet JL (2009) Water transport in epoxy-aliphatic amine networks. Influence of curing cycles. *Eur Polym J* 45:1524–1534
10. Merdas I, ThomINETTE F, Tcharkhtchi A, Verdu J (2002) Factors governing water absorption by composite matrices. *Compos Sci Technol* 62:487–492
11. Adamson MJ (1980) Thermal expansion and swelling of cured epoxy resin used in graphite/epoxy composite materials. *J Mater Sci* 15:1736–1745
12. Enns JB, Gilham JK (1983) Effect of the extent of cure on the modulus, glass transition, water absorption, and density of an amine-cured epoxy. *Appl Polym Sci* 28(9):2831–2846
13. Gupta VB, Drzal LT, Rich M (1985) The physical basis of moisture transport in a cured epoxy resin system. *J Appl Polym Sci* 30(11):4467–4693
14. Johncock P, Tudgey GF (1986) Some effects of structure, composition and cure on the water absorption and glass transition temperature of amine-cured epoxies. *Brit Polym J* 18(5): 292–302
15. Van Krevelen DW, Te Nijenhuis K (2009) Properties of polymers. Their correlation with chemical structure. Their numerical estimation and prediction from additive group contributions, 4th edn. Elsevier, Amsterdam
16. Small PA (1953) Some factors affecting the solubility of polymers. *J Appl Chem* 3(2):71–80
17. Van Krevelen DW (1965) Chemical structure and properties of coal. XXVIII. Coal constitution and solvent extraction. *Fuel* 44(4):229–242
18. Hoy KL (1970) New values of the solubility parameters from vapor pressure data. *J Paint Techn* 42(541):76–118
19. Fedors RF (1974) A method for estimating both the solubility parameters and molar volumes of liquids. *Polym Eng Sci* 14:147–154
20. Barrie JA (1968) Water in polymers. In: Crank J, Park GS (eds) Diffusion in polymers, Chap. 8, Academic Press, London, pp 259–314
21. Gaudichet-Maurin E, ThomINETTE F, Verdu J (2008) Water sorption characteristics in moderately hydrophilic polymers, Part 1: Effect of polar groups concentration and temperature in water sorption in aromatic polysulfones. *J Appl Polym Sci* 109(5):3279–3285
22. Courvoisier E (2017) Analysis and kinetic modeling of the thermal ageing of PEI and PEEK matrices and its consequences on water absorption. PhD thesis, Arts et Métiers ParisTech, Paris, March 2017

23. Baschek G, Hartwig G, Zahradnik F (1999) Effect of water absorption in polymers at low and high temperatures. *Polymer* 40:3433–3441
24. ThomINETTE F, Gaudichet-Maurin E, Verdu J (2008) Effect of structure on water diffusion in moderately hydrophilic polymers. *Defect Diffus Forum* 258(260):442–446
25. Carter HG, Kibler KG (1978) Langmuir-type model for anomalous moisture diffusion in composite resins. *J Compos Mater* 12(2):118–131
26. Cai LW, Weitsman Y (1994) Non-Fickian moisture diffusion in polymeric composites. *J Compos Mater* 28(2):130–154
27. Brethous R, Colin X, Fayolle B, Gervais (2016) Non-Fickian behavior of water absorption in an epoxy-amidoamine network. *AIP Conf Proc* 1736: paper no. 020070
28. Serpe G, Chaupart Verdu J (1997) Ageing of polyamide 11 in acid solutions. *Polymer* 38 (8):1911–1917
29. El Mazry C, Correc O, Colin X (2012) A new kinetic model for predicting polyamide 6-6 hydrolysis and its mechanical embrittlement. *Polym Degrad Stab* 97(6):1049–1059
30. Li L, Yu Y, Wu Q, Zhang G, Li S (2009) Effect of chemical structure on the water sorption of amine-cured epoxy resins. *Corros Sci* 51(12):3000–3006